Multiscale simulations reveal the driving forces underlying V337M-induced Tau core fragment aggregation

Pengxuan Xia[a], Yujie Chen[b], Jiaxing Tang[c], Lulu Guan[a], Dushuo Feng[a], and Yu Zou[a]*

[a] Department of Sport and Exercise Science, College of Education, Zhejiang University, Hangzhou, Zhejiang 310058, P. R. China

[b] College of Mathematics and Physics, Shanghai University of Electric Power, Shanghai 200090, China

[c] School of Physical Education, Xiangnan University, Chenzhou 423000 Hunan, China

This material contains temperature lists and convergence assessments of REMD simulations, two supplementary tables (Tables S1-S2) and five supplementary figures (Figures S1-S8).

Table S1. The temperature (K) list used in the 48-replica REMD simulations of PHF6** in WT system.

308	310.24	312.5	314.77	317.05	319.34	321.64	323.96
326.28	328.62	330.97	333.33	335.65	338.03	340.43	342.84
345.27	347.7	350.15	352.61	355.08	357.57	360.07	362.58
365.1	367.64	370.19	372.78	375.36	377.95	380.55	383.16
385.79	388.44	391.09	393.76	396.44	399.14	401.85	404.58
407.32	410.08	412.85	415.63	418.43	421.25	424.08	425

Table S2. The temperature (K) list used in the 48-replica REMD simulations of PHF6** in V337M system.

308	310.26	312.54	314.83	317.12	319.43	321.75	324.09
326.43	328.79	331.16	333.54	335.93	338.32	340.74	343.17
345.62	348.07	350.54	353.02	355.51	358.02	360.54	363.08
365.63	368.18	370.76	373.34	375.94	378.55	381.11	383.75
386.4	389.07	391.74	394.44	397.14	399.87	402.6	405.23
407.99	410.77	413.56	416.37	419.19	422.03	424.88	425

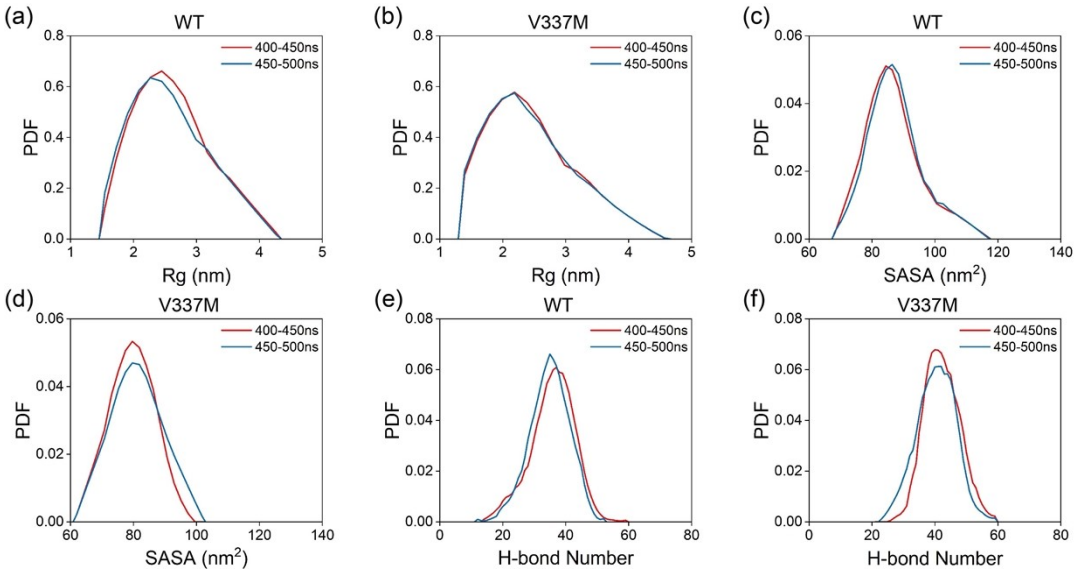

Fig. S1 Probability distribution function (PDF) of the Rg (a, b), SASA (c, d), H-bond number (e, f) of PHF6** oligomers in the WT and V337M systems in REMD runs with two different time intervals (400-450 ns and 450-500 ns).

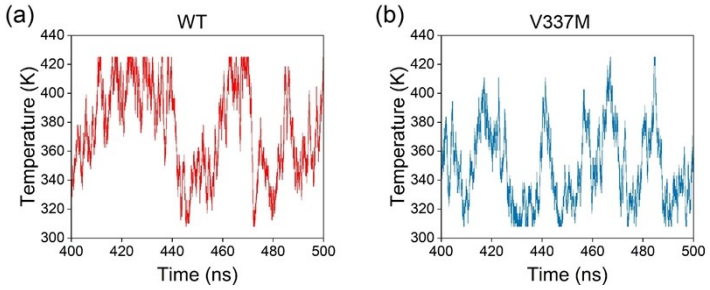

Fig. S2 The time evolution of temperature swapping of one representative replica in temperature space for WT and V337M system.

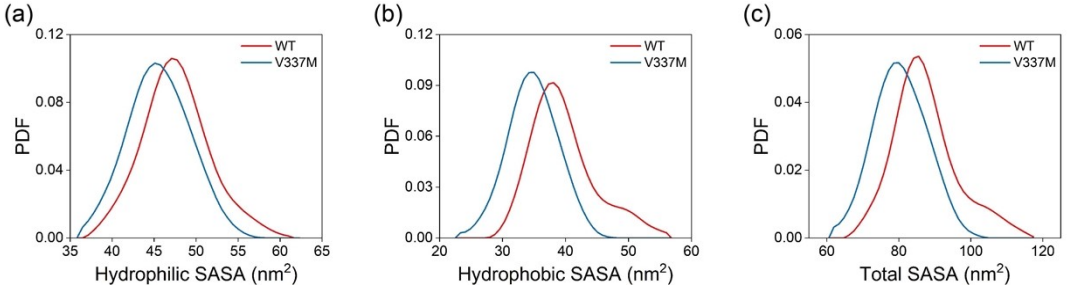

Fig. S3 PDF of the Hydrophilic (a), Hydrophobic (b), and total (c) SASA of PHF6** oligomers in

the WT and V337M systems. The distributions were obtained from REMD simulations using the 400-500ns trajectories.

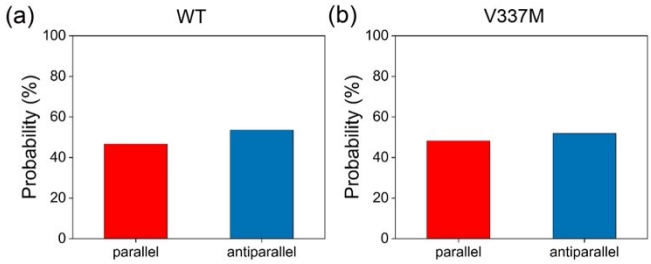

Fig. S4. Population analysis of β-sheet registry in WT and V337M PHF6** oligomers from CMD simulations. (a, b) Probabilities of parallel and antiparallel β-sheet arrangements in the WT and V337M systems, respectively, calculated from the interchain β-sheet registry analysis of the CMD trajectories. An interchain β-sheet pair was defined as a chain pair in which both peptides contained at least two consecutive β-strand residues and simultaneously formed at least one interchain backbone hydrogen bond and one intermolecular contact. The relative orientation of each β-sheet pair was classified as parallel or antiparallel according to the angle between the strand direction vectors of the two peptide chains. The reported probabilities represent the fractions of parallel and antiparallel β-sheet pairs among all classified interchain β-sheet pairs.

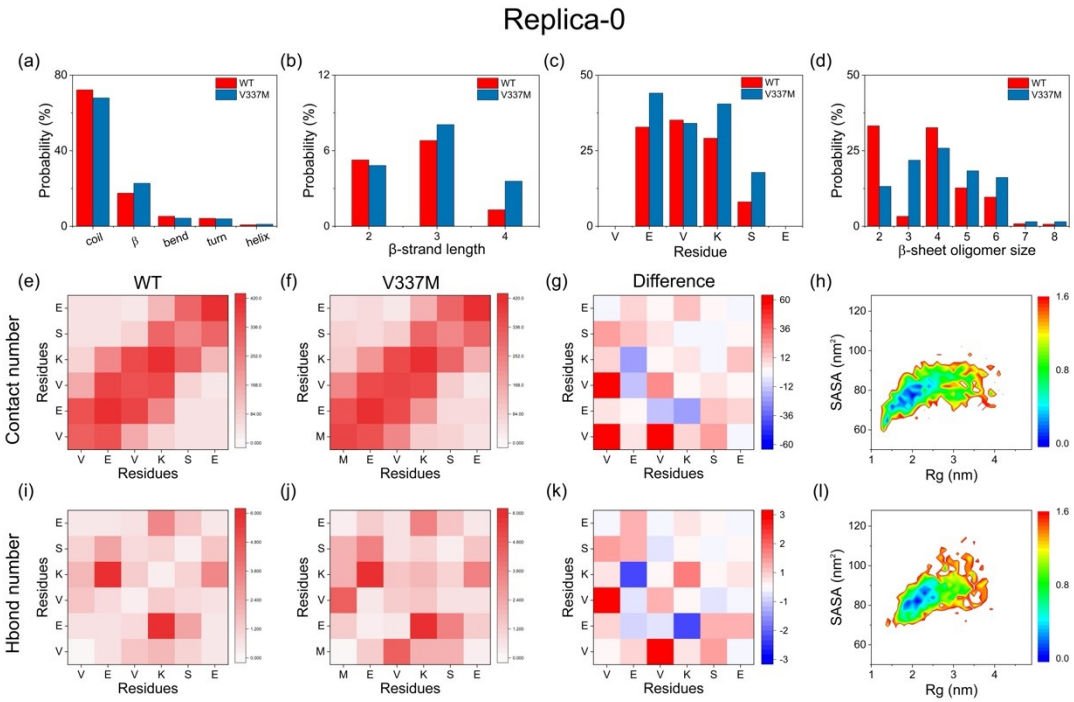

Fig. S5. REMD analysis of PHF6** oligomers in the WT and V337M systems from Replica-0 (308 K). (a) Representative molecular structures of the PHF6** hexapeptide in the WT and V337M systems. Probabilities of β-strand length (b), Residue-wise β-sheet (c) and β-sheet oligomer size (d) for the WT and V337M systems. (e, f) Residue-residue contact maps in the WT and V337M systems. (g) Contact map difference obtained by subtracting the WT contact number from those of the V337M system. (i, j) Residue-residue H-bond maps for the WT and V337M systems. (k) H-bond map difference between the V337M and WT systems. Two-dimensional PMF of WT (h) and V337M (l) systems as a function of Rg and SASA.

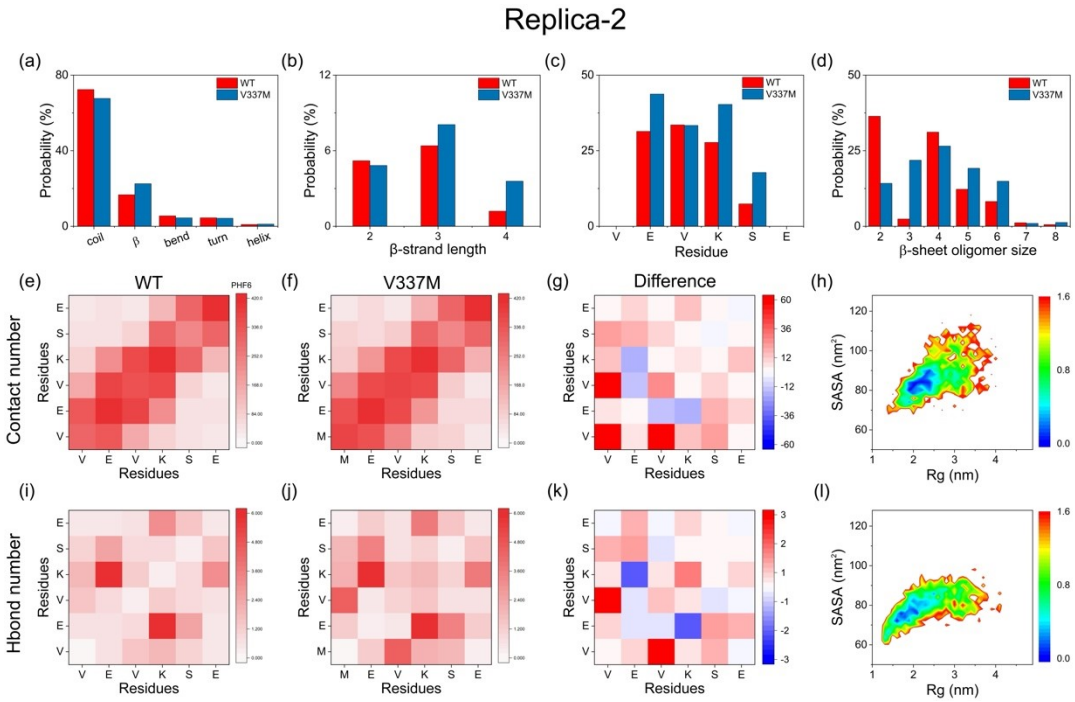

Fig. S6. REMD analysis of PHF6** oligomers in the WT and V337M systems from Replica-2 (312.5 K). (a) Representative molecular structures of the PHF6** hexapeptide in the WT and V337M systems. Probabilities of β-strand length (b), Residue-wise β-sheet (c) and β-sheet oligomer size (d) for the WT and V337M systems. (e, f) Residue-residue contact maps in the WT and V337M systems. (g) Contact map difference obtained by subtracting the WT contact number from those of the V337M system. (i, j) Residue-residue H-bond maps for the WT and V337M systems. (k) H-bond map difference between the V337M and WT systems. Two-dimensional PMF of WT (h) and V337M (l) systems as a function of Rg and SASA.

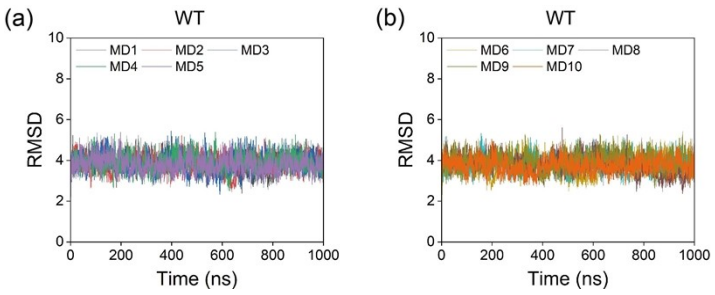

Fig. S7 Time evolution of RMSD from ten independent simulations of the WT system.

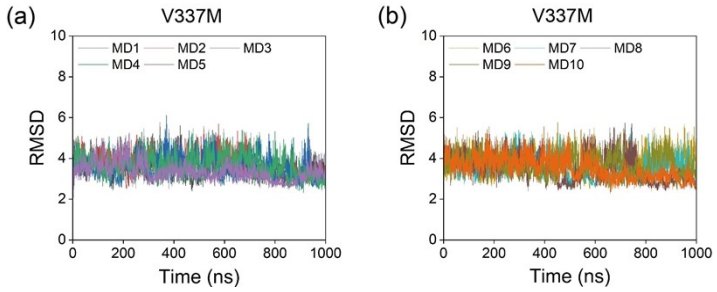

Fig. S8 Time evolution of RMSD from ten independent simulations of the V337M system.